Magnetic hourglass dispersion and its relation to high-temperature superconductivity in iron-tuned $Fe_{1+y}Te_{0.7}Se_{0.3}$

2012 New J. Phys. 14 073025

(http://iopscience.iop.org/1367-2630/14/7/073025)

New Journal of Physics
The open-access journal for physics

Magnetic hourglass dispersion and its relation to high-temperature superconductivity in iron-tuned $Fe_{1+y}Te_{0.7}Se_{0.3}$

N Tsyrulin[1], R Viennois[2,3], E Giannini[3], M Boehm[4], M Jimenez-Ruiz[4], A A Omrani[1], B Dalla Piazza[1] and H M Rønnow[1,5]

[1] Laboratory for Quantum Magnetism, École Polytechnique Fédérale de Lausanne (EPFL), CH-1015 Lausanne, Switzerland
[2] Institut Charles Gerhardt Montpellier, Université Montpellier II, F-34095 Montpellier, France
[3] DPMC, University of Geneva, 24 Quai E Ansermet, 1211 Geneva, Switzerland
[4] Institut Laue Langevin, 6 rue Jules Horowitz BP156, 38024 Grenoble Cedex 9, France
E-mail: henrik.ronnow@epfl.ch

New Journal of Physics **14** (2012) 073025 (9pp)
Received 22 March 2012
Published 12 July 2012
Online at http://www.njp.org/
doi:10.1088/1367-2630/14/7/073025

Abstract. High-temperature superconductivity remains arguably the greatest enigma of condensed matter physics. The discovery of iron-based high-temperature superconductors [1, 2] has renewed the importance of understanding superconductivity in materials susceptible to magnetic order and fluctuations. Intriguingly, they show magnetic fluctuations reminiscent of superconducting (SC) cuprates [3], including a 'resonance' and an 'hourglass'-shaped dispersion [4], which provides an opportunity to gain new insights into the coupling between spin fluctuations and superconductivity. In this paper, we report inelastic neutron scattering data on $Fe_{1+y}Te_{0.7}Se_{0.3}$ using excess iron concentration to tune between an SC ($y = 0.02$) and a non-SC ($y = 0.05$) ground state. We find incommensurate spectra in both the samples but discover that in the one that becomes SC, a constriction toward a commensurate hourglass-shape develops well above T_c. Conversely, a spin gap and a concomitant spectral weight

[5] Author to whom any correspondence should be addressed.

shift happen below T_c. Our results imply that the hourglass-shaped dispersion is most likely a prerequisite for superconductivity, whereas the spin gap and shift of spectral weight are the consequences of superconductivity. We explain this observation by pointing out that an inward dispersion toward the commensurate wave vector is needed for the opening of a spin gap to lower the magnetic exchange energy and hence provide the necessary condensation energy for the SC state to emerge.

Essentially, most families of superconducting (SC) cuprates display a common spin excitation spectrum with a spin resonance, an hourglass-shape dispersion and a spin gap below T_c. This magnetic hourglass dispersion is quite unusual and seems to be almost concomitant with high-temperature superconductivity, although a few non-SC examples were reported recently [5]. However, despite intensive debate based on extensive theoretical and experimental efforts, the answer to a key question remains elusive: what is the relation between the hourglass and the SC transition—and which is the consequence of the other? Surprisingly, the recently discovered iron-based superconductors display remarkable similarities in the magnetic excitation spectrum, strongly suggesting a common mechanism of superconductivity. In iron–arsenic-based compounds as well as in the iron chalcogenides, the emergence of superconductivity is accompanied by the opening of a spin gap and appearance of a commensurate 'spin resonance' and 'hourglass'-shaped magnetic dispersion, which have been observed in several inelastic neutron scattering experiments [6–8]. We have discovered that tuning superconductivity in iron chalcogenide by small amounts of excess iron provides fresh insight into the mechanism of SC.

$Fe_{1+y}Te_{0.7}Se_{0.3}$ displays the simplest single-layered crystal structure among the iron-based superconductors. The excess of iron located on an interstitial site strongly influences both magnetic and SC properties as a tuning parameter in addition to the Te/Se ratio [9–11]. For our experiments, two batches of $Fe_{1+y}Te_{0.7}Se_{0.3}$ were grown by the Bridgman–Stockbarger method with starting Fe : (Te, Se) ratios of 1 : 1 and 0.9 : 1, respectively. Precursors were heated to $T = 930\,^{\circ}C$ in quartz tubes and then slowly cooled. Structure refinement of small single crystals determined that the iron contents y is $y = 0.05$ and $y = 0.02$ for the two batches, respectively. This difference in iron content was confirmed by energy-dispersive x-ray spectroscopy (EDX) analysis. More details can be found in [10].

Superconductivity was determined by the Meissner effect in magnetization measurements on single crystals of $Fe_{1.05}Te_{0.7}Se_{0.3}$ and $Fe_{1.02}Te_{0.7}Se_{0.3}$ with masses of 7.4(1) and 8.1(1) mg, respectively. Measurements were carried out with magnetic field applied along the crystallographic c-axis after zero-field cooling (ZFC) or field cooling (FC). At $\mu_0 H = 2\,\mathrm{mT}$, a sharp drop in ZFC magnetization in the $y = 0.02$ sample demonstrates bulk superconductivity developing between $T_c^{\mathrm{onset}} = 10.8\,\mathrm{K}$ and $T_c^{\mathrm{bulk}} = 9.7\,\mathrm{K}$ (figure 1(a)). The sharpness of the transition witnesses high sample homogeneity and quality, which may explain the sharpness of our inelastic data compared to previous studies on larger crystals. In contrast, the $y = 0.05$ sample shows essentially no Meissner effect (figure 1(b)). Compared to $y = 0.02$, the very small decrease in ZFC magnetization of 0.03 emu (mole Oe)$^{-1}$ implies that any SC volume fraction in our $Fe_{1.05}Te_{0.7}Se_{0.3}$ sample is smaller than 0.1%. Thus we have successfully prepared two high-quality samples with the same Se content and a controlled small Fe content tuning the system from a homogenous bulk superconductor at $y = 0.02$ to a completely non-SC sample at $y = 0.05$.

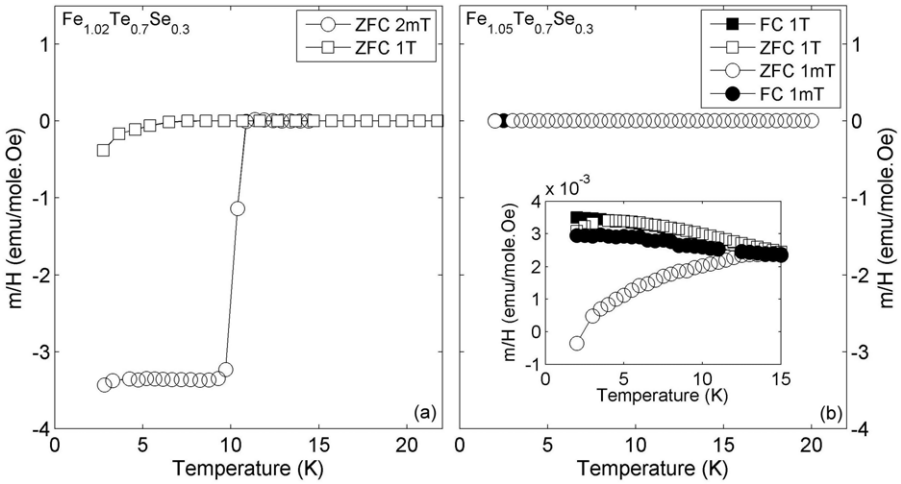

Figure 1. Magnetization of $Fe_{1.02}Te_{0.7}Se_{0.3}$ and $Fe_{1.05}Te_{0.7}Se_{0.3}$ measured as a function of temperature is shown in (a) and (b), respectively. White and black circles show the result of low-field ZFC and FC measurements, respectively. White and black squares indicate the results of ZFC and FC measurements made at $\mu_0 H = 1\,\mathrm{T}$.

The spin dynamics in both samples was investigated using the thermal neutron three-axis spectrometer IN8 at the Institut Laue-Langevin, France. Three single crystals with iron content $y = 0.02$ with a total mass of $m = 0.85(3)$ g were co-aligned with a total mosaic spread of less than 0.7°. A single crystal $y = 0.05$ with a mass $m = 0.63(1)$ g was used for the measurements. Both samples were fixed on aluminum holders. The reciprocal plane $(h, k, 0)$ of both compounds was co-aligned with the horizontal scattering plane of the spectrometer. The measurements were carried out using a standard ^{4}He Orange cryostat in the temperature range $2\,\mathrm{K} \leqslant T \leqslant 40\,\mathrm{K}$. Using (002) Bragg reflection from a pyrolithic graphite (PG) analyzer, the final energy of neutrons was set to $E_\mathrm{f} = 14\,\mathrm{meV}$. We used PG(002) as a monochromator and double focusing mode of the spectrometer. Such a configuration resulted in the energy and the wave-vector resolution of $\Delta E \approx 1\,\mathrm{meV}$ and $\Delta Q \approx 0.063\,\mathrm{\AA}^{-1}$, respectively, which were measured by performing an energy scan through an incoherent position and a wave-vector (Q-) scan across a nuclear Bragg peak, respectively. The measured intensity was normalized to the incident flux monitor.

Our inelastic neutron scattering measurements revealed steeply dispersing magnetic excitations at positions $(1/2 \pm \delta, 1/2 \mp \delta, 0)$ in both the samples. The peak widths exceed the instrumental resolution, in agreement with observations in related materials [12]. The dispersion was mapped by performing constant energy scans as summarized in figure 2. Each scan was fitted by two Gaussians symmetrically placed around (1/2, 1/2, 0). The resulting peak positions are indicated as points on top of the colormaps.

Starting from the non-SC $y = 0.05$ sample, at $T = 40\,\mathrm{K}$ the incommensuration $\delta = 0.154(14)$, and the intensity is essentially energy independent up to 10 meV. This value of δ and the dispersion above $E = 10\,\mathrm{meV}$ are consistent with previous papers [12–15]. Lowering the temperature to $T = 2\,\mathrm{K}$ has a minor influence on the incommensuration, and no commensurate signal was detected in this sample up to $E = 35\,\mathrm{meV}$. At $T = 40\,\mathrm{K}$, the

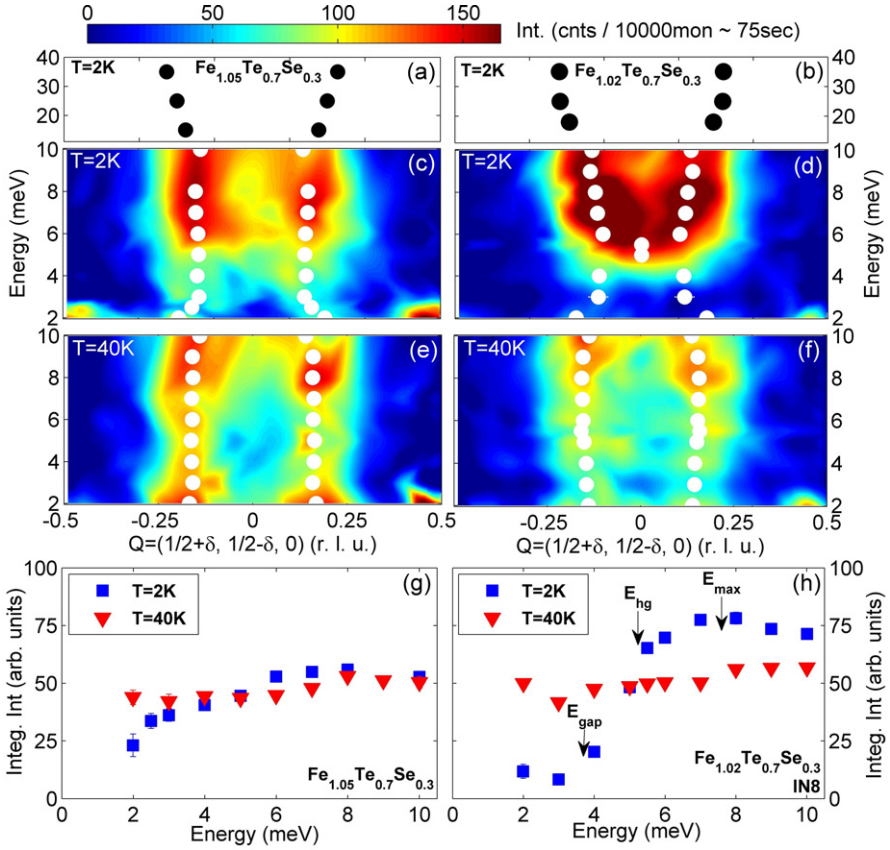

Figure 2. Magnetic spectrum and dispersion along $(1/2+\delta, 1/2-\delta, 0)$ at $y = 0.05$ (a, c, e) and $y = 0.02$ (b, d, f) from Q-scans at a series of energies. Colormaps represent intensity with a Q-independent background subtracted. Below 2 meV, the incoherent elastic background becomes dominant. Data above $E = 10$ meV were measured at different configurations, and intensities are not directly comparable. Each scan was fitted by two symmetric Gaussians, yielding the dispersion (circles) and integrated intensity, which are shown in (g, h) as a function of energy. Blue and red circles correspond to $T = 2$ K and $T = 40$ K, respectively.

$y = 0.02$ sample displays a very similar incommensuration. However, lowering the temperature to $T = 2$ K reveals dramatic differences: (i) Q-scans at $E = 5$ meV and $E = 5.5$ meV narrow down into a single commensurate peak defining $E_{\rm hg} = 5.3(5)$ meV; (ii) spectral weight is removed below $E_{\rm hg}$ and shifted to above $E_{\rm hg}$. This dramatic restructuring of the magnetic excitation spectrum is direct experimental evidence for an intricate coupling between magnetism and superconductivity, and is very reminiscent of the behavior in cuprate superconductors, with one noticeable difference: in $Fe_{1.02}Te_{0.7}Se_{0.3}$ the spectrum is completely incommensurate at high temperature and becomes commensurate upon lowering the temperature. In the cuprates the hourglass-shape was thought to persist at all temperatures, and our discovery calls for an investigation versus temperature, e.g. in underdoped $La_{2-x}Sr_xCuO_4$.

Our data are consistent with those reported previously for SC $FeSe_{0.4}Te_{0.6}$ and 'nearly superconducting' (NSC) $FeSe_{0.45}Te_{0.55}$ [4]. In SC $FeSe_{0.4}Te_{0.6}$, a constriction toward

commensuration was also observed at $E = 4.5$ meV when the temperature is lowered from $T = 20$ to $T = 1.5$ K. It is also possible that the sample would show complete incommensurability at $T = 40$ K. In [4], the NSC data were interpreted to also be showing an hourglass dispersion, which led to the conclusion that it is not directly associated with superconductivity. However, with the new insight provided by our non-SC $Fe_{1.05}Te_{0.7}Se_{0.3}$ data, the NSC data of [4] can be reassessed to be consistent with our interpretation. Indeed at $T = 15$ K, there is no discernible commensuration at $E = 4.5$ meV, and there is little—if any—commensuration upon lowering the temperature to $T = 4$ K. The reason why our non-SC sample displays a sharper, clearly incommensurate spectrum may be that it is completely non-SC, much smaller (0.63 g compared to 23 g in [4]), and therefore likely to be more homogeneous. The NSC sample in [4] had up to 30% SC volume fraction.

Compared to the cuprates, we argue that three characteristic energies must be defined: E_{gap}, below which spectral weight is depleted in the SC state; E_{max}—the energy where a maximum in intensity develops in the SC state; and E_{hg}, the energy where the incommensurate spectrum constricts toward the commensurate wave vector, thereby forming an hourglass-shape. In both $La_{2-x}Sr_xCuO_4$ and YBCO—the two cuprate families most studied by inelastic neutron scattering—there are incommensurate excitations with an 'hourglass'-shaped dispersion toward the commensurate point at E_{hg} about $E = 40$ meV [16, 17]. In $La_{2-x}Sr_xCuO_4$, the spin gap E_{gap} that opens upon entering the SC state is only about $E = 8$ meV at optimal doping, and spectral weight is redistributed along the incommensurate parts of the excitations, such that a maximum in intensity occurs at an incommensurate resonance around $E_{max} = 18$ meV $\sim 2E_{gap}$ [18, 19]. The maximum in intensity is hence the consequence of shifting weight from below the gap. Whereas E_{gap} and E_{max} are therefore two manifestations of the same feature, in $La_{2-x}Sr_xCuO_4$ the commensurate energy of the hourglass dispersion E_{hg} is independent of this. In YBCO on the other hand, the energy scale of E_{gap} is higher, such that the redistribution of spectral weight falls around the commensurate energy such that E_{max} and E_{hg} tend to coincide into a pronounced commensurate 'resonance' peak.

To quantify the details of the spectral weight restructuring, we plot in figures 2(g) and (h) the integrated magnetic intensity extracted from Gaussian fits to the constant energy scans. For $y = 0.05$, the intensity is almost energy independent. The slight difference between $T = 40$ and $T = 2$ K is consistent with $1 - e^{-E/k_BT}$, implying an essentially temperature-independent dynamic susceptibility. For $y = 0.02$, the $T = 40$ K intensity has a similar weak energy dependence, but the $T = 2$ K intensity shows a sharp spin gap of $E_{gap} = 3.7(5)$ meV, with only a weak intensity remaining below. It can be seen that the spectral weight removed from low energy is shifted to energies above E_{hg}, creating a maximum at $E_{max} = 7.5(5)$ meV. There is less increase in the Q-integrated intensity at the commensurate position $E_{hg} = 5.3(5)$ meV, where the increase in peak intensity at the commensurate position comes from the merging in Q of two incommensurate peaks, and not from energies below or above E_{hg}. In this respect the behavior of $Fe_{1.02}Te_{0.7}Se_{0.3}$ with $E_{hg} \lesssim E_{max}$ is more akin to YBCO with $E_{hg} \simeq E_{max}$ than to $La_{2-x}Sr_xCuO_4$ with $E_{hg} > E_{max}$.

The temperature dependence of the spectral restructuring was studied by performing Q-scans at a constant energy $E = 5.5$ meV and energy scans at $Q = (1/2, 1/2, 0)$. Figure 3(a) shows Q-scans fitted by Gaussian peaks with a linear background. For clarity we plot the fit curves separately in figure 3(b). Importantly, the peaks already start shifting toward the commensurate position at $T = 15$ K, well above T_c and the commensuration is almost complete already at $T = 10\,\text{K} \simeq T_c$, with little subsequent change down to $T = 3.5$ K. The colorplot

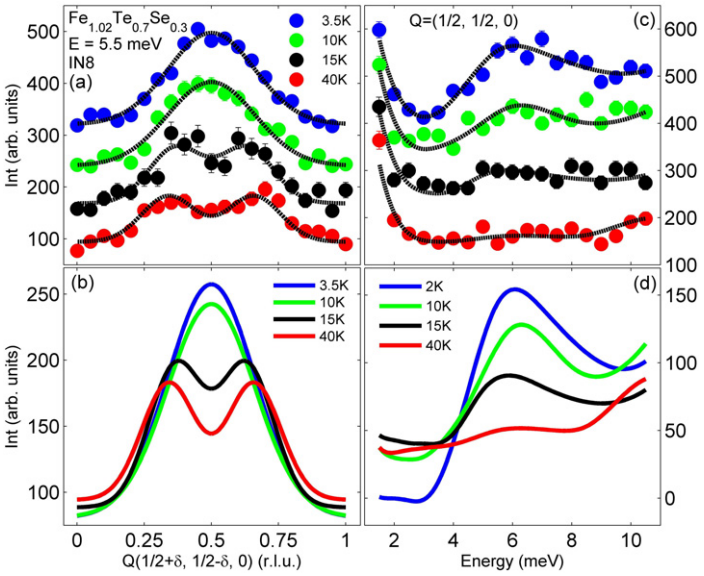

Figure 3. (a) Scans at a constant $E = 5.5$ meV for $T = 3.5$, $T = 10$, $T = 15$ and $T = 40$ K are shown by red, black, green, brown and blue circles, respectively. For clarity, scans are displaced vertically. Black lines are fits to two Gaussians symmetric around (1/2, 1/2, 0). (b) Comparison of the fits results for each temperature. (c) Constant Q-scans performed at $Q = (1/2, 1/2, 0)$ at $T = 2$, $T = 10$, $T = 15$ and $T = 40$ K. For clarity, scans are displaced vertically. The lines are smooth curves aiding the comparison between temperatures. (d) The smooth curves are compared for different temperatures, with the tail from the elastic line removed.

in figure 4(a) shows the complete evolution of the Q-scan performed at $E_{hg} = 5.3$ meV in the temperature range from $T = 50$ to $T = 2.5$ K. These data together with those shown in figures 2(d) and (f) clearly illustrate the process of commensuration toward an hourglass-shape dispersion as a function of temperature. The constriction toward commensuration at $E_{hg} = 5.3$ meV clearly develops above T_c. This is further documented in figure 4(b), showing how the full-width at half-maximum of the double-peak structure at $E_{hg} = 5.3$ meV decreases continuously from $T = 40$ to $T = 2.5$ K with a majority of the commensuration happening before T_c.

In contrast, the energy scans displayed in figures 3(c) and (d) show a different temperature dependence for the spin gap $E_{gap} = 3.7$ meV. Below $E = 3.7$ meV, the intensity remains constant from $T = 40$ to $T = 10$ K, and only below T_c does the intensity suddenly drop. This is also seen in a temperature scan at $E = 3$ meV (figure 4(c)), which shows a very different temperature dependence than figure 4(b), with a kink to rapid depletion of intensity below T_c. The weak decrease above T_c may be accounted for by proximity to the 5.3 meV commensuration, or a fluctuating precursor to the gap. Hence, the spin gap opens sharply below T_c. Combined with the fact that superconductivity is absent in $Fe_{1.05}Te_{0.7}Se_{0.3}$, in which the magnetic spectrum remains incommensurate at all temperatures, the implications of our observations are that the commensurate hourglass-shape at E_{hg} of the magnetic spectrum is most likely a prerequisite for superconductivity, whereas the spin gap is the consequence of

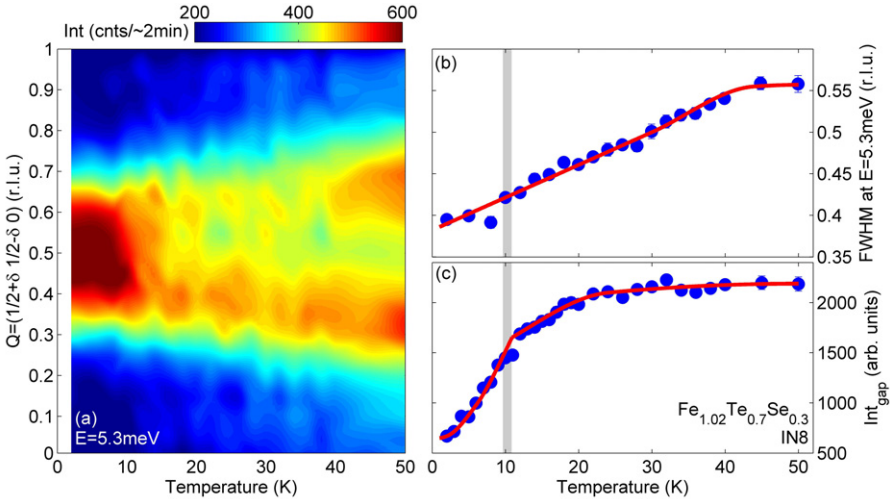

Figure 4. (a) The temperature evolution of a constant energy scan at $E = 5.3$ meV is shown as a colormap. The figure was obtained by merging and smoothing 21 Q-scans in the temperature range of $T = 2.5$–50 K in total. (b) Temperature dependence of the full-width at half-maximum of Q-scans at a constant $E = 5.3$ meV. A shift toward the commensurate center point happens gradually from 40 K and below. The red line is a guide to the eye. (c) Intensity at $E = 3$ meV below E_{gap} as a function of temperature. A pronounced onset of depletion of the intensity sets in below T_{c}, consistent with the opening of a gap, whereas there is only a weak temperature dependence above T_{c}. The red line is a guide to the eye.

superconductivity, and the concomitant maximum in intensity at E_{max} is in turn a consequence of the spin gap.

The observation that the hourglass dispersion seems a necessary condition for superconductivity supports that the SC condensation energy can come from the change in magnetic exchange energy between the normal state and the SC state [20, 21]. Based on arguments from the t–J model, whose essence should be extendable to the Fe-based system, the change in exchange energy can be written as $\Delta E_{\mathrm{ex}} = 2J(\langle \mathbf{S}_i \cdot \mathbf{S}_j \rangle_{\mathrm{S}} - \langle \mathbf{S}_i \cdot \mathbf{S}_j \rangle_{\mathrm{N}})$ (S and N refer to the SC and normal states, respectively), which can be expressed as a momentum weighted integral of the dynamical structure factor, which is proportional to neutron intensity:

$$\langle \mathbf{S}_i \cdot \mathbf{S}_j \rangle = 3J \int \frac{\mathrm{d}\omega}{\pi} \int \frac{\mathrm{d}2q}{(2\pi)^2} S(\mathbf{q}, \omega)(\cos(q_x) + \cos(q_y)). \tag{1}$$

The momentum weight factor is optimal at $\mathbf{q} = (\pi, \pi)$, which implies that shifting the spectral weight from incommensurate positions toward the commensurate position lowers the magnetic exchange energy. As sketched in figure 5, opening a spin gap would increase the exchange energy in a system with excitations dispersing away from the commensurate point, leave the exchange energy unchanged in a system with energy-independent incommensurate fluctuations (such as our $Fe_{1.05}Te_{0.7}Se_{0.3}$ sample), but would lower the exchange energy for systems showing inward dispersion from incommensurate wave vectors toward the commensurate point (such as our $Fe_{1.02}Te_{0.7}Se_{0.3}$ sample).

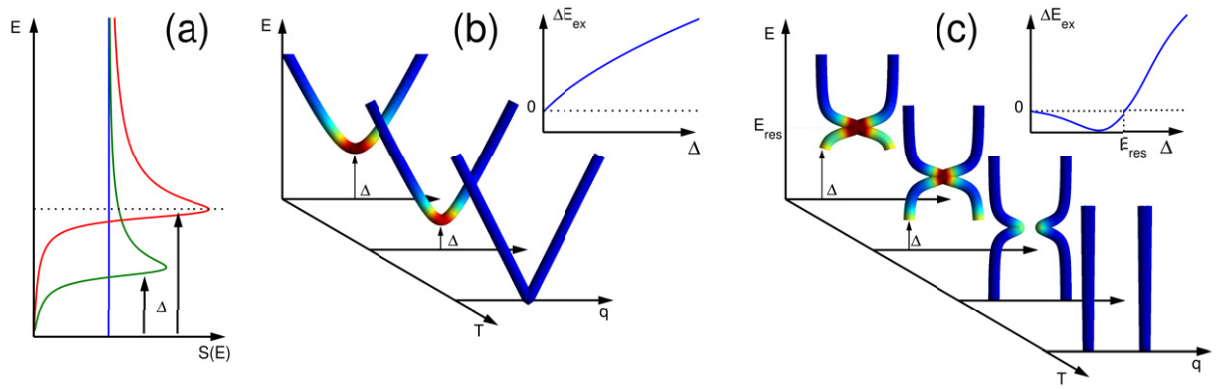

Figure 5. Sketch of how opening an energy gap in the spin excitation spectrum changes the magnetic exchange energy ΔE_{ex}. (a) The energy-dependent scattering function $S(E)$, which for a two-dimensional antiferromagnet is constant in the absence of a gap. When the gap opens, the spectral weight is shifted from below the gap to above the gap. (b) Opening a gap in a conventional linear dispersion shifts spectral weight away from the commensurate (π, π) point and would increase ΔE_{ex} (inset). (c) Opening a gap in an hourglass dispersion shifts spectral weight toward $q = (\pi, \pi)$, and creates a minimum in ΔE_{ex} for Δ just below E_{res}.

The recent observation of an hourglass dispersion with $E_{hg} = 14\,\text{meV}$ in insulating, non-SC $La_{5/3}Sr_{1/3}CoO_4$ [22] shows that it is not a sufficient condition for high-temperature superconductivity. Rather, it places an upper limit on the spin gap and hence on the SC transition temperature, since opening a spin gap larger than E_{hg} would shift the spectral weight back away from (π, π). Both copper oxide- and Fe-based systems—including our sample—obey $E_{gap} \simeq 4k_B T_c$ (except for highly under-doped cuprates, where E_{gap} is further reduced due to the softening of the d-wave SC gap around the nodal point [23]). A similar attempt at scaling $E_{hg} \simeq 5.3k_B T_c$ holds for YBCO and $Fe_{1.02}Te_{0.7}Se_{0.3}$, where the spin gap is squeezed up toward E_{hg}, but breaks down, e.g., for the $La_{2-x}Sr_xCuO_4$ family where other effects must suppress T_c and hence E_{gap}.

We therefore conclude that the existence of an hourglass-shaped dispersion is a necessary condition for high-temperature superconductivity of the nature found in iron- and copper oxide-based materials. This implies that the mechanism for superconductivity is a lowering of the magnetic exchange energy through a shifting of spectral weight toward the commensurate point, and we conjecture that the energy E_{hg} of the commensurate point in this hourglass dispersion imposes a maximum possible transition temperature $T_c^{max} \simeq E_{hg}/5.3k_B$. If a new family of high-temperature superconductors is discovered, measuring E_{hg} will provide an estimate of the maximum achievable T_c and hence provide important guidance as to whether further compositional exploration within that family may be futile or fruitful.

Acknowledgments

We acknowledge useful discussions with N B Christensen, B Normand and D J Scalapino. This work was supported by the Swiss National Science Foundation and MaNEP. Preliminary neutron scattering measurements were made at SINQ, PSI, Switzerland.

References

[1] Kamihara Y, Watanabe T, Hirano M and Hosono H 2008 *J. Am. Chem. Soc.* **130** 3296
[2] Ren Z-A *et al* 2008 *Europhys. Lett.* **82** 57002
[3] Tranquada J M 2007 Neutron scattering studies of antiferromagnetic correlations in cuprates *Handbook of High-Temperature Superconductivity: Theory and Experiment* ed J R Schrieffer and J S Brooks (New York: Springer) p 257
[4] Li S *et al* 2010 *Phys. Rev. Lett.* **105** 157002
[5] Ulbric H *et al* 2011 arXiv:1112.1799v1 [cond-mat.str-el]
[6] Johnston D C 2010 *Adv. Phys.* **59** 803
[7] Lumsden M D and Christianson A D 2010 *J. Phys.: Condens. Matter* **22** 203203
[8] Inosov D S *et al* 2010 *Nature Phys.* **6** 178
[9] Liu T J *et al* 2009 *Phys. Rev.* B **80** 174509
[10] Viennois R, Giannini E, van der Marel D and Cerny R 2010 *J. Solid State Chem.* **183** 769
[11] Bendele M *et al* 2010 *Phys. Rev.* B **82** 212504
[12] Argyriou D N *et al* 2010 *Phys. Rev.* B **81** 220503
[13] Qiu Y *et al* 2009 *Phys. Rev. Lett.* **103** 067008
[14] Wen J *et al* 2010 *Phys. Rev.* B **81** 100513
[15] Babkevich P *et al* 2010 *J. Phys.: Condens. Matter* **22** 142202
[16] Vignolle B *et al* 2007 *Nature Phys.* **3** 163
[17] Reznik D *et al* 2004 *Phys. Rev. Lett.* **93** 207003
[18] Christensen N B *et al* 2004 *Phys. Rev. Lett.* **93** 147002
[19] Tranquada J M *et al* 2004 *Phys. Rev.* B **69** 174507
[20] Scalapino D J and White S R 1998 *Phys. Rev.* B **58** 8222
[21] Woo H *et al* 2006 *Nature Phys.* **2** 600
[22] Boothroyd A T, Babkevich P, Prabhakaran D and F P G 2011 *Nature* **471** 341
[23] Chang J *et al* 2007 *Phys. Rev. Lett.* **98** 077004